*Journal of Engineering Mathematics* **43:** 57–74, 2002.


# Green functions for initial free-surface flows due to 3D impulsive bottom deflections

T. MILOH[1], P. A. TYVAND[2] and G. ZILMAN[1]
[1]*Faculty of Engineering, Tel Aviv University, Ramat Aviv 69978, Israel*
[2]*Department of Agricultural Engineering, Agricultural University of Norway, 1432 Aas, Norway*

Received 25 January 2001; accepted in revised form 7 January 2002

**Abstract.** The immediate impulsive flow of an incompressible fluid due to a concentrated flux through an otherwise impermeable boundary is investigated analytically in three dimensions. The flow is inviscid and irrotational, and obeys the equipotential condition at the free surface, which is initially horizontal. Various elementary bottom geometries are analyzed: rectangular basins, sloping beaches, semi-cylindrical and hemispherical basins. Special attention is paid to the case of impulsive free-surface flows generated on a uniform sloping beach. A general integral solution is presented and compared against a series solution found for a discrete set of angles. The results are relevant for the modeling of tsunami generation due to rapid bottom deflections.

**Key words:** bottom deflection, green function, impulsive free-surface flows, sloping beach, tsunami generation

## 1. Introduction

The present paper is devoted to three-dimensional free-surface flows forced by impulsive bottom deflections. The considered limit of very rapid bottom deflection means that this process takes place during a time interval much shorter than the gravitational time scale. In this limit, where gravity can be neglected, the free surface will be at rest after the bottom deflection has ceased, and the equipotential condition may be applied at the initially horizontal free surface. This deformed surface is then released from rest, serving as the initial value in a three-dimensional Cauchy-Poisson like problem. If a rapid normal deflection of the bottom is specified, the resulting surface elevation can be obtained from the present theory, by assuming that linear theory is valid. This can be done by integrating up in time the fluid velocity normal to the free surface. Such a model is relevant for studying the early stages of tsunami generation. A similar study of two-dimensional flows has been published in [1]. The present paper is only concerned with the initial flow governed by the equipotential condition at the free surface. But it is also possible to follow the evolution in time analytically by using a small-time expansion. Such an analysis for a nonlinear problem has been carried out in a number of works [2]–[7] related to submerged sources/sinks. A corresponding 3D initial free-surface problem due to a submerged spherical explosion, formulated as a mixed boundary-value problem has been recently solved by [8]. For a sloping beach a 2D gravity dependent Green function has been considered in [9] and [10].

The structure of the paper is as follows. In Section 2 we formulate the general linear boundary-value problem and define the so-called impulsive free-surface velocity Green function. It is then showed how one can relate the initial free-surface elevation to an arbitrary impulsive bottom deflection of the basin. In Section 3 we present some particular analytic solutions of Green functions for some selected geometries which consist of plain boundaries.

These Green functions should not be confused with the traditional gravity dependent Green function which has been extensively investigated in the past (see for example [11], and others). In Section 4 we consider in some detail the case of a sloping beach. First, using the Kontorovich-Lebedev integral representation, we give a general solution which is valid for any slope. Then, we compare it with the solution obtained from the method of successive images found for some particular slope angles, namely $\alpha = \pi/2n$, where $n$ is an integer. It is proven analytically that these two independent solutions are indeed identical. Also obtained are asymptotic solutions for the wave elevation which hold for small slope angles and near the shore line, where the water depth tends to zero. We conclude the analytic part of the paper by including two practical cases which involve curved boundaries: a semi-circular geometry which corresponds to an infinitely long half filled circular pipe and a semi-spherical shape which models a half-filled spherical container.

## 2. Formulation of the general problem

We consider the free-surface flow generated by a volume flux $Q$ through a finite area $A$ located on an impermeable rigid boundary. The fluid is inviscid, incompressible and its motion is irrotational. A Cartesian coordinate system $Oxyz$ is introduced, with the $Oxy$ plane taken in the undisturbed free surface, whereas the $z$ axis points vertically upwards.

We define the total volume flux as:

$$Q(t) = \int\int_A q(x, y, z, t)\, \mathrm{d}A, \tag{1}$$

where $q(x, y, z, t)$ is the discharge of a surface point source depending on time $t$.

The velocity potential $\Phi(x, y, z, t)$ satisfies Laplace's equation

$$\nabla^2 \Phi = 0, \tag{2}$$

and the following boundary condition on the rigid boundaries:

$$\frac{\partial \Phi}{\partial n} = \begin{cases} 0 & (x, y, z) \notin A \\ q & (x, y, z) \in A \end{cases}, \tag{3}$$

where **n** is the normal to the rigid boundary at the location of the source and directed into the fluid.

The full nonlinear boundary conditions at the free surface are:

$$\frac{\partial \eta}{\partial t} + \nabla \Phi \cdot \nabla \eta = \frac{\partial \Phi}{\partial z}, \quad z = \eta(x, y, t) \tag{4}$$

$$\frac{\partial \Phi}{\partial t} + \frac{1}{2}|\nabla \Phi|^2 + gz = 0, \quad z = \eta(x, y, t), \tag{5}$$

where the surface elevation is denoted by $\eta(x, y, t)$.

It is assumed here that the forcing of boundary flux occurs during a short time interval $t_0$ which is much smaller than the gravitational time scale $T$:

$$t_0 \ll T, \qquad T = \sqrt{H/g}, \tag{6}$$

where $H$ denotes the characteristic submergence of the source, and $g$ is the acceleration of gravity. A basic requirement for linearizing the free-surface boundary condition is as follows [1]:

$$\int_0^{t_0} Q(t)\,\mathrm{d}t \ll H^3. \tag{7}$$

It represents all of the bottom which is subject to nonzero flux. Since the up-welling region for the impulsive source flow at the free surface has a length scale $H$ both in $x$ and $y$ direction, we see that the inequality (7) means that the surface peak is much shorter than the dominating wavelength. This is the usual linearization condition for water waves, and it is well satisfied for tsunami generation at typical ocean depths [12]. Thus, when the requirements (6) and (7) are satisfied, the boundary conditions (4) and (5) can be linearized to give the infinite-frequency limit of linearized water-wave theory [13]:

$$\frac{\partial \eta}{\partial t} = \frac{\partial \Phi}{\partial z}, \quad z = 0, \tag{8}$$

$$\Phi(x, y, 0, t) = 0, \quad 0 < t < t_0. \tag{9}$$

The problem formulated in (2) and (8)–(9) is linear. Thus, the layout geometry, the strength of the sources, and the impulsive Green function $G(x, y, z; x_0, y_0, z_0)$ define the general solution:

$$\Phi(x, y, z, t) = \frac{1}{2\pi} \int\int_A G(x, y, z; x_0, y_0, z_0) q(x_0, y_0, z_0, t)\,\mathrm{d}A. \tag{10}$$

The impulsive Green function $G(x, y, z; x_0, y_{0,}z_0)$ is defined in the lower half plane $z < 0$ by the boundary value problem

$$\nabla^2 G = 0, \tag{11}$$

$$G(x, y, 0; x_0, y_0, z_0) = 0, \tag{12}$$

$$\frac{\partial G}{\partial n} = 2\pi\delta(x - x_0)\delta(y - y_0)\delta(z - z_0) \quad \text{on} \quad A \tag{13}$$

and a proper decay at infinity. This Green function can be represented as a sum of the singular and regular parts as follows:

$$G = -\frac{1}{R^-} + H, \tag{14}$$

where

$$R^- = \sqrt{(x - x_0) + (y - y_0)^2 + (z - z_0)^2}, \tag{15}$$

and $H(x, y, z; x_0, y_0, z_0)$ is a regular harmonic function satisfying the boundary conditions (12) and (13). Integrating up the linearized kinematic condition (8) we get the expression for the free-surface elevation:

$$\eta(x, y, t) = \frac{1}{2\pi} \int\int_A W(x, y; x_0, y_0, z_0) \chi(x_0, y_0, z_0, t)\,\mathrm{d}A, \tag{16}$$

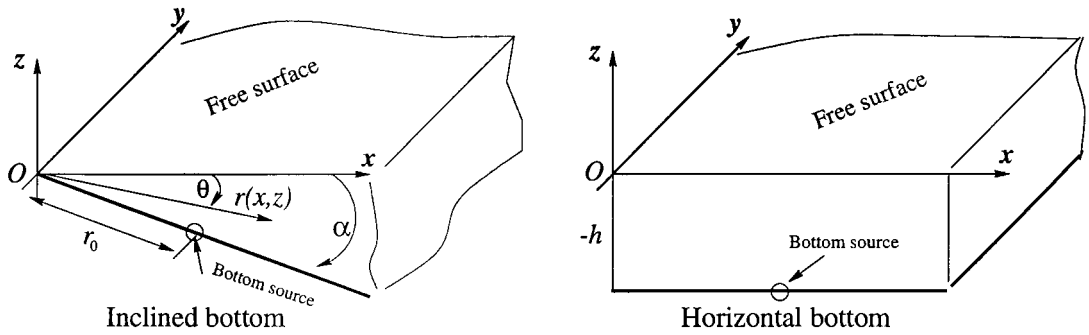


*Figure 1.* System of coordinates and general notations.

where

$$\chi(x, y, z, t) = \int_0^t q(x, y, z, \tau)\, \mathrm{d}\tau \tag{17}$$

and

$$W(x, y; x_0, y_0, z_0) = \frac{\partial}{\partial z} G(x, y, z; x_0, y_0, z_0)\Big|_{z=0}. \tag{18}$$

The function $W$ is named here as the impulsive free-surface velocity Green function. It is defined by two scaling parameters namely, the source strength scaling parameter $Q_0$ and some typical length scale $L$. Thus, the dimensionless free-surface velocity Green function $\zeta$ can be represented as:

$$\zeta = \frac{W}{Q_0/L^2}. \tag{19}$$

The choice of the relevant length scale depends on the particular problem, and is a matter of convenience. For instance, considering an infinitely deep water bounded by a vertical wall, $L$ must be identified as the submergence depth of the wall source. In the case of an infinite deep water, bounded by two vertical walls, it may be pertinent to choose the characteristic length as a distance between the walls rather than the submergence of the source. In the case of a sloping beach the characteristic length can be defined along the bottom as a distance of the source from the waterline (see Figures 1–3). Herein, in each particular situation we explain the physical meaning of the typical length scale.

## 3. Green function: particular cases

For some particular geometries the Green function can be constructed by using certain images of the basic singularity in such a way that the required boundary condition on the free surface and rigid boundaries are satisfied. Only seven representative cases are illustrated in this section. For the sake of brevity we omit the detailed derivations of the expressions for the Green functions $G$ and give only the final results for the free surface velocity Green function $W$.

• *Uniform layer of constant depth h*. The source with coordinates $(0, 0, -h)$ is located on the bottom (Figure 2a):

$$W(x, y; 0, 0, -h) = \sum_{n=-\infty}^{\infty} \frac{(-1)^n (2n-1)h}{\left[x^2 + y^2 + (2n-1)^2 h^2\right]^{3/2}}. \tag{20}$$

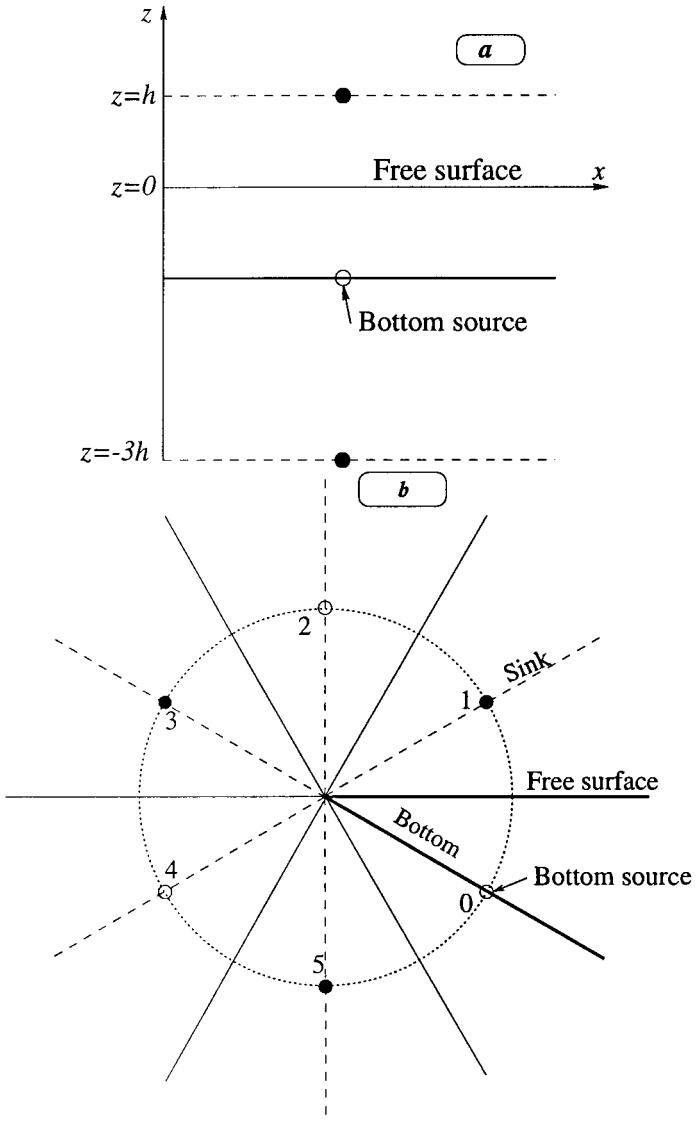


*Figure 2.* System of the base source and its corresponding images: a) – horizontal bottom; b) – inclined bottom, $\alpha = \pi/2n$, $(n = 1, 2, \dots)$; here $n = 3$.

• *Beach with slope angle* $\alpha = \pi/2l$, ($l$–integer). The source with coordinates $(r_0 \cos\alpha, 0, -r_0 \sin\alpha)$ is located on the slope (Figure 2b):

$$W(x, y; r_0 \cos\alpha, 0, -r_0 \sin\alpha) = \sum_{n=0}^{2l-1} \frac{(-1)^n r_0 \sin(2n+1)\alpha}{\left[x^2 + r_0^2 + y^2 - 2x r_0 \cos(2n+1)\alpha\right]^{3/2}}. \tag{21}$$

• *Two parallel vertical walls separated by a distance* $b$. The source with coordinates $(0, 0, z_0)$ is located on a wall (Figure 3a):

$$W(x, y; 0, 0, z_0) = -\sum_{n=-\infty}^{\infty} \frac{2z_0}{\left[(x+2nb)^2 + y^2 + z_0^2\right]^{3/2}}. \tag{22}$$

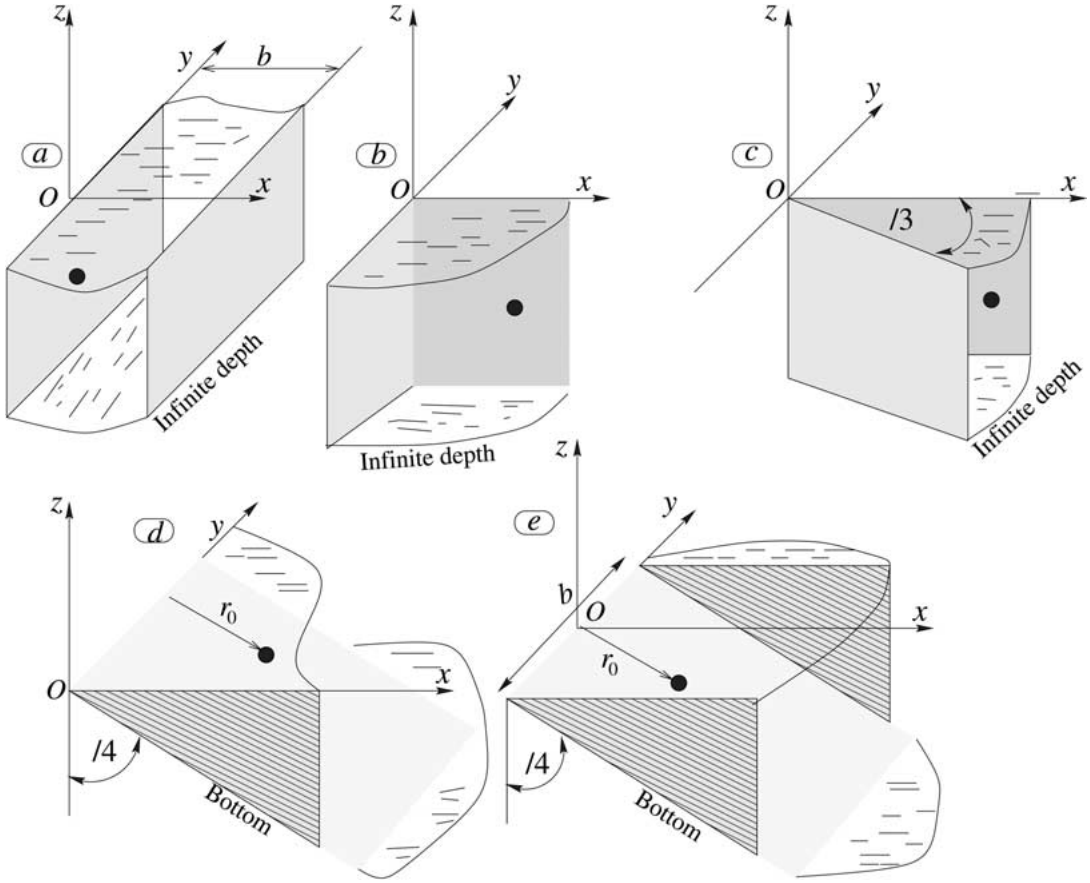


*Figure 3.* Particular cases which can be obtained by summation of images of the base source.

• *Two vertical walls intersecting at a right angle*. The source with coordinates $(x_0, 0, z_0)$ is located on a wall (Figure 3b):

$$W(x, y; x_0, 0, z_0) = -\sum_{n=0}^{1} \frac{2(-1)^n z_0}{\left\{[x + (-1)^n x_0]^2 + y^2 + z_0^2)\right\}^{3/2}}. \tag{23}$$

• *A vertical wall making an angle $\pi/3$ with another vertical wall*. The source with coordinates $(x_0, 0, z_0)$ is located on a wall (Figure 3c):

$$\begin{aligned} W(x, y; x_0, 0, z_0) = & -\frac{2z_0}{\left[(x - x_0)^2 + y^2 + z_0^2\right]^{3/2}} \\ & -\sum_{n=0}^{1} \frac{2z_0}{\left\{(x + x_0/2)^2 + [y + (-1)^n \sqrt{3} x_0/2]^2 + z_0^2\right\}^{3/2}} \end{aligned} \tag{24}$$

• *Beach with slope angle $\pi/4$ along the wall*. The source with coordinates $(r_0/\sqrt{2}, y_0, -r_0/\sqrt{2})$ is located on the slope (Figure 3d):

$$W(x, y; r_0/\sqrt{2}, y_0, -r_0/\sqrt{2}) = -\sum_{n=0}^{1}\sum_{m=0}^{1} \frac{(-1)^n\sqrt{2}r_0}{\left\{\left[x+(-1)^n r_0/\sqrt{2}\right]^2+\left[y+(-1)^m y_0\right]^2 + r_0^2/2\right\}^{3/2}}. \tag{25}$$

• *Beach with slope angle $\pi/4$ between two walls of distance $b$ apart*. The source with coordinates$(r_0/\sqrt{2}, 0, -r_0/\sqrt{2})$ is located on the slope (Figure 3e):

$$W(x, y; r_0/\sqrt{2}, 0, -r_0/\sqrt{2}) = -\sum_{n=0}^{1}\sum_{m=-\infty}^{\infty} \frac{(-1)^n\sqrt{2}r_0}{\left\{[x + (-1)^n r_0\sqrt{2}]^2 + (y + mb)^2 + r_0^2/2\right\}^{3/2}}. \tag{26}$$

For the case of a uniform depth $h$ (Equation (20), Figure 2a) the free-surface velocity Green function can be represented also as an integral:

$$W(x, y; 0, 0, -h) = \int_0^\infty \lambda \operatorname{sech} \lambda h \, J_0(\lambda\sqrt{x^2 + y^2}) \, \mathrm{d}\lambda, \tag{27}$$

where $J_0$ is the Bessel function. By expanding $\operatorname{sech}\lambda h$ into series of powers of $\exp(-\lambda h)$ and by a consequent analytic integration of (27) we can show that the integral (27) and the series (20) are identical [14, Appendix 1].

### 3.1. Numerical example

As illustrative examples, expressions (22) and (26) were calculated numerically and compared in Tables 1–2 with the corresponding two-dimensional solutions for a two-dimensional source of unit strength. For the case (22) the two-dimensional limit can be written as [6]:

$$W_{2D}(y; 0, z_0) = -\frac{2z_0}{y^2 + z_0^2} \tag{28}$$

and

$$W_{2D}^0 \equiv W_{2D}(y; 0, z_0)|_{y=0} = -\frac{2}{z_0} \tag{29}$$

For the case (26) the corresponding series converges towards the following solution given in [1], for $r_0 \gg 1$:

$$W_{2D}(x; r_0/\sqrt{2}) = \frac{2\pi\xi^{\pi/2\alpha-1}}{\alpha r_0(1 + \xi^{\pi/\alpha})}, \tag{30}$$

where $\xi = x/r_0$, and $\alpha = \pi/4$. For the simple case $\xi = 1$, (30) yields:

$$W_{2D}^0 = W_{2D}(x; r_0/\sqrt{2})\Big|_{x=r_0} = \frac{4}{r_0}. \tag{31}$$

It should be noted that the obtained series of images may exhibit slow convergence. Although it can be improved [11], we do not discuss here this numerical aspect. Employing a double precision arithmetic (16 digits), allow us to perform the illustrative calculations without any special difficulties.

The convergence of the three-dimensional solutions into the two-dimensional asymptotic limit solutions can be interpreted as a corresponding Saint-Venant principle for a potential

*Table 1.* Free-surface velocity for a wall source of strength $Q_0$ located in a channel of infinite depth and width $b$: Equation (22), Figure 3a. For different submergence depths of the source, we give the exact velocity, and its two-dimensional asymptotic limit. The velocity is evaluated at the same horizontal position as that of the source. The infinite series solution has been truncated after 999 terms

| $z_0/b$ | $W^0_{2D}b/Q_0$ | $Wb^2/Q_0$ |
|---|---|---|
| −0·5 | 4·0000 | 8·2779 |
| −1·0 | 2·0000 | 2·4523 |
| −2·0 | 1·0000 | 1·0124 |
| −3·0 | 0·66667 | 0·6671 |
| −4·0 | 0·5000 | 0·5000 |

*Table 2.* Free-surface velocity for a bottom source of strength $Q_0$ located in the centerplane of a channel of width $b$ with a bottom slope $\pi/4$: Equation (26), Figure 3e. For different locations of the source $r_0$, we give the exact velocity, and its two-dimensional asymptotic limit for $x = r_0$. The infinite series solution (26) has been truncated after 100 terms

| $r_0/b$ | $W^0_{2D}b/Q_0$ | $Wb^2/Q_0$ |
|---|---|---|
| 1·0 | 4·0000 | 6·1775 |
| 2·0 | 2·0000 | 2·1175 |
| 3·0 | 1·3333 | 1·3417 |
| 4·0 | 1·0000 | 1·0006 |

flow. This principle is well-known in elasticity theory [15, p. 131], where it tells us that the torsion field in a slender beam is governed by the integrated inhomogeneity (the net torque) applied at its ends. The details of the shear stress distribution at the ends of a slender beam do not matter at distances more than five cross section diameters, and only the net torque matters.

In the present flow problem, the inhomogeneity (*i.e.*, the source causing the flow) which is distributed over the channel width, will influence the solution only as an integrated quantity (total source flux) at distances of the order of several length units.

## 4. Uniform beach with arbitrary slope

### 4.1. Green function

We will now consider a uniform beach with a constant slope $\alpha$ (Figure 1). As above, we take the source to be situated in the $x, z$ plane, at a distance $r_0$ down the slope. Introducing cylindrical coordinates

$$x = r\cos\theta, \quad z = -r\sin\theta, \tag{32}$$

we can write the governing equation for the regular potential as follows:

$$\frac{1}{r}\frac{\partial}{\partial r}\left(r\frac{\partial H}{\partial r}\right) + \frac{1}{r^2}\frac{\partial^2 H}{\partial \theta^2} + \frac{\partial^2 H}{\partial y^2} = 0. \tag{33}$$

The particular solution $H_{k\tau}(r, y, \theta)$ of this equation which is bounded for $r = 0$ and $r \to \infty$ is the following [16]:

$$H_{k\tau} = K_{i\tau}(kr)\begin{Bmatrix}\cosh\ \tau\theta \\ \sinh\ \tau\theta\end{Bmatrix}\begin{Bmatrix}\sin ky \\ \cos ky\end{Bmatrix}, \tag{34}$$

for given $k$ and $\tau$, where $K_\nu$ denotes the modified Bessel function of the second kind and of order $\nu$.

Recalling that the general solution is written as (14), and noting that on the beach (except at the source point)

$$\frac{\partial}{\partial n}\left(\frac{1}{R^-}\right) = 0, \tag{35}$$

it follows that the regular potential $H$ obeys the condition (3) of zero normal velocity at the slope, *i.e.*,

$$\frac{\partial H}{\partial \theta} = 0, \quad \theta = \alpha. \tag{36}$$

This allows us to construct the general solution satisfying (36) in the form of the Kontorovich-Lebedev integral:

$$H(r, y, \theta; r_0, 0, \alpha) = \frac{2}{\pi}\int_0^\infty \int_0^\infty A(k,\tau)\,\frac{\cosh[(\alpha-\theta)\tau]}{\cosh(\alpha\tau)}\cos ky\; K_{i\tau}(kr)\;\mathrm{d}k\;\mathrm{d}\tau, \tag{37}$$

where $A(k, \tau)$ is to be determined from the boundary conditions. Use of the equipotential boundary condition (11) at $z = 0$ ($\theta = 0$) gives the expression:

$$\frac{2}{\pi}\int_0^\infty \int_0^\infty A(k,\tau)\; K_{i\tau}(kx)\;\cos\, ky\;\mathrm{d}\tau\;\mathrm{d}k = \frac{1}{\sqrt{(x-x_0)^2+y^2+z_0^2}}. \tag{38}$$

Thus, applying to (38) the Fourier cosine transform we find:

$$\int_0^\infty A(k,\tau)K_{i\tau}(kx)\;\mathrm{d}\tau = \int_0^\infty \frac{\cos\, ky}{\sqrt{(x-x_0)^2+y^2+z_0^2}}\,\mathrm{d}k = K_0\left[k\sqrt{(x-x_0)^2+y^2+z_0^2}\right]. \tag{39}$$

Following [16], the above integral equation can be inverted analytically, leading to:

$$A(k,\tau) = \frac{2}{\pi}\cosh[(\pi-\alpha)\tau]K_{i\tau}(kr_0), \tag{40}$$

where $r_0^2 = x_0^2 + z_0^2$. Finally, we end up with the following expression for the Green function:

$$\begin{aligned} G(x, y, z; x_0, 0, z_0) = & -\frac{1}{\sqrt{r^2+r_0^2+y^2-2rr_0\cos(\alpha-\theta)}} \\ & +\frac{2}{\pi}\int_0^\infty\int_0^\infty \frac{\cos\tau s\cosh[(\pi-\alpha)\tau]\cosh[(\alpha-\theta)\tau]}{\cosh\alpha\tau\sqrt{r^2+r_0^2+y^2+2rr_0\cosh s}}\,\mathrm{d}\tau\;\mathrm{d}s. \end{aligned} \tag{41}$$

An alternative form of this Green function, which will be used below, can be obtained by invoking the following relation [16]:

$$\int_0^\infty \frac{\cos\tau s\;\mathrm{d}s}{\sqrt{r^2+r_0^2+y^2+2rr_0\cosh s}} = \frac{1}{\sqrt{2rr_0}\sinh\pi\tau}\int_\lambda^\infty \frac{\sin\tau s\;\mathrm{d}s}{\sqrt{\cosh s-\cosh\lambda}}, \tag{42}$$

where

$$\cosh\lambda = \frac{r^2+y^2+r_0^2}{2rr_0}. \tag{43}$$

It finally leads to:

$$H = \frac{2}{\pi\sqrt{2rr_0}}\int_\lambda^\infty \frac{\mathrm{d}s}{\sqrt{\cosh s-\cosh\lambda}}\int_0^\infty \frac{\cosh[(\alpha-\theta)\tau]\cosh[(\pi-\alpha)\tau]}{\sinh\pi\tau\cosh\alpha\tau}\sin\tau s\mathrm{d}\tau \tag{44}$$

which is used for further analytic calculations.

### 4.2. Surface velocity Green function

By invoking (44), the surface velocity Green function $W$ is defined as:

$$W = \frac{\partial}{\partial z}\left(-\frac{1}{R^-}\right)\Big|_{z=0} + \frac{2}{\pi x\sqrt{2xr_0}}\int_\lambda^\infty \frac{\mathrm{d}s}{\sqrt{\cosh\, s - \cosh\,\lambda}} \times \int_0^\infty \frac{\tau \sinh\,\alpha\tau\ \cosh[(\pi-\alpha)\tau]}{\sinh\,\pi\tau\ \cosh\,\alpha\tau}\sin\,\tau s\ \mathrm{d}\tau. \tag{45}$$

Consider first the inner integral in (45) which can be represented as

$$I = \frac{1}{2}\mathrm{Im}\int_{-\infty}^{\infty} f(\tau)\mathrm{e}^{\mathrm{i}s\tau}\mathrm{d}\tau, \tag{46}$$

where

$$f(\tau) = \tau\frac{\sinh\alpha\tau}{\cosh\alpha\tau}\frac{\cosh[(\pi-\alpha)\tau]}{\sinh\pi\tau}. \tag{47}$$

This integral can be calculated explicitly. For this purpose we choose the contour of integration in the upper complex half-plane $\psi = \tau + \mathrm{i}\tau_1$ along the real axis, along the semi-circle of infinitely large radius which connects the ends of the real axis, and along the semi-circle of infinitely small radius in the center at the origin of the real and complex axes (Figure 4a). Since $\lim_{\tau\to 0} f(\tau) = 0$ and $\lim_{\tau\to\infty} f(\tau) = 0$ it follows from Jordan and Cauchy theorems that the integrals along the semi-circles vanish, and that the integral along the real axis is equal to the sum of the residues inside the chosen contour multiplied by $2\pi\mathrm{i}$.

To calculate the residues we note that in the complex plane $\psi$ the integrand (47) has single poles at the roots of the equations:

$$\sinh\pi\tau = 0,\ \ \tau_k = \mathrm{i}k,\ \ k = (1, 2, \dots), \tag{48}$$

$$\cosh\alpha\tau = 0,\ \ \tau_n = \frac{2n+1}{2\alpha}\pi\mathrm{i},\ \ (n = 0, 1, \dots). \tag{49}$$

It should be noted that for some particular angles $\alpha = (2n+1)\pi/k$, the singularities inside the contour of integration may not be isolated. However, we tacitly assume that these points are excluded from consideration.

The integral $I$ can be represented as a sum of two integrals, $I = I_k + I_n$, where the subscripts relate to the roots $\tau_k$ and $\tau_n$, correspondingly. After calculating the residues, we obtain:

$$I_k = -\sum_{k=1}^{\infty} k\ \mathrm{e}^{-ks}\sin k\alpha, \tag{50}$$

$$I_n = \frac{\pi^2}{2\alpha^2}\sum_{n=0}^{\infty}(-1)^n(2n+1)\mathrm{e}^{-(2n+1)\frac{\pi s}{2\alpha}}. \tag{51}$$

These series can be calculated in a closed form [17, Equation 5.4.12], which gives:

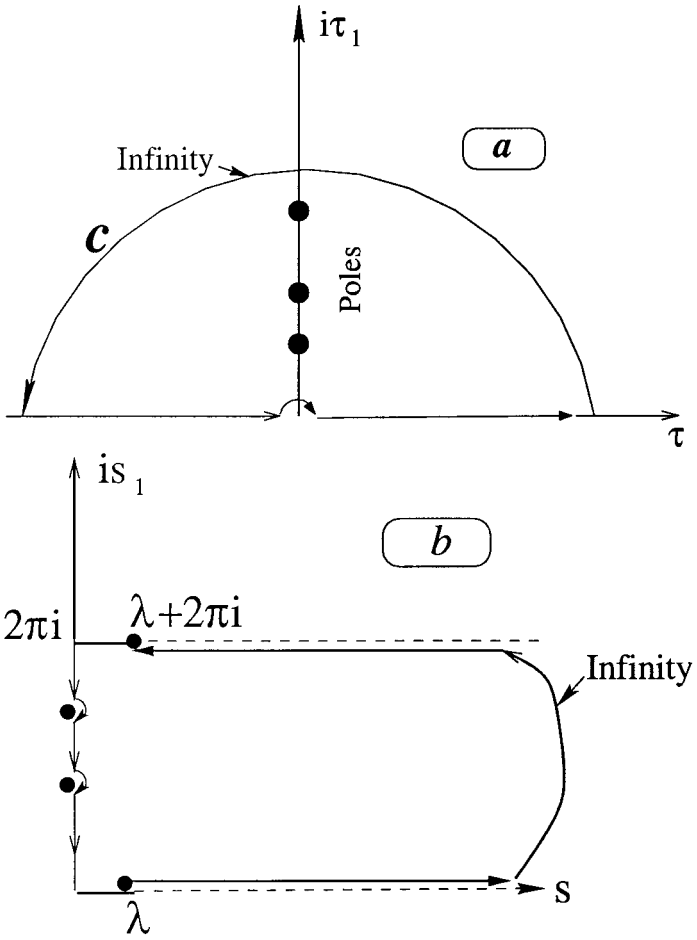


*Figure 4.* Contours of integration.

$$I_k = \frac{\sin\alpha}{2}\frac{\sinh s}{(\cosh s - \cos\alpha)^2}, \tag{52}$$

$$I_n = \frac{\pi^2}{4\alpha^2}\frac{\sinh(\pi s/2\alpha)}{\cosh^2(\pi s/2\alpha)}. \tag{53}$$

Substituting (52) and (53) in (45) and performing one analytic integration we obtain the following expression for the impulsive free-surface velocity Green function for a uniform sloping beach:

$$W = \frac{\pi}{2x\sqrt{2xr_0}\alpha^2}\int_\lambda^\infty \frac{\sinh(\pi s/2\alpha)}{\cosh^2(\pi s/2\alpha)}\frac{\mathrm{d}s}{\sqrt{\cosh s - \cosh\lambda}}. \tag{54}$$

This result is continuous with respect to $\alpha$, therefore it is valid for any $0 < \alpha \leq \pi$.

### 4.3. PARTICULAR CASE $\alpha = \pi/2l$, ($l$-INTEGER)

Consider next the integral

$$B = \int_{\lambda}^{\infty} \frac{\sinh(\pi s/2\alpha)}{\cosh^2(\pi s/2\alpha)} \frac{\mathrm{d}s}{\sqrt{\cosh s - \cosh\lambda}} \tag{55}$$

taken in the complex plane $s + is_1$ along the contour $C$ which is shown in Figure 4b. Its integrand has second-order poles on the imaginary axis at points which are defined by the roots of the equation:

$$\cosh\frac{\pi s}{2\alpha} = 0, \qquad s_m = \frac{2m+1}{2l}\pi i, \ (m = 0, 1, \dots). \tag{56}$$

These poles are surrounded by semi-circles of infinitely small radius. Each integral along the semi-circle is equal to the residue in the pole multiplied by $-\pi\mathrm{i}$. Since the imaginary poles are located within the range $\Im\mathrm{m}\, s_m \le 2\pi$, it follows that the number of poles inside the contour is finite and less than $2l - 1$. On the imaginary axis (excluding the poles) the integral is imaginary. It is also imaginary on the intervals $[0, \lambda]$ and $[2\pi\mathrm{i}, \lambda + 2\pi\mathrm{i}]$, correspondingly. Since the hyperbolic function has a period $2\pi i$, the integrals on the lower cut $(\lambda + \mathrm{i}0, \infty + \mathrm{i}0)$ and the upper cut $[\infty + 2\pi(\mathrm{i} - 0)]$, $\lambda + 2\pi(\mathrm{i} - 0)$ are equal. This allows us to represent the integral $B$ as:

$$B = \frac{\pi\mathrm{i}}{2} \sum_{m=0}^{2l-1} \mathrm{Res}|_{s=s_m}\,. \tag{57}$$

Calculating these residues leads to

$$\mathrm{Res}|_{s=s_m} = \frac{-1}{2\beta^2} \frac{\sinh\gamma}{(\cosh\gamma - a)^{3/2}\sinh\beta\gamma}\bigg|_{\substack{\gamma=(2m+1)\alpha\mathrm{i} \\ \beta=\pi/2\alpha}}, \tag{58}$$

and, thus, (54) can be written as the following sum

$$W = \frac{1}{2x\sqrt{2xr_0}} \sum_{m=0}^{2l-1} \frac{(-1)^m \sin(2m+1)\alpha}{[\cosh\lambda - \cos(2m+1)\alpha]^{3/2}}. \tag{59}$$

It can be easily seen that the two independent expressions, *i.e.*, (21) obtained by the method of images, and (59) which is calculated as a particular case of the more general solution, are identical.

### 4.4. Asymptotic expressions of the surface velocity Green function

For $\lambda/\alpha \gg 1$ it follows that $\exp(-\pi\lambda/2\alpha) \ll 1$. In such a case the expression for the free surface Green function (59) can be calculated in a closed form [18, Equation 4.9.23]:

$$W = \frac{1}{x\sqrt{2xr_0}} \frac{\pi}{\alpha^2} \int_{\lambda}^{\infty} \frac{\exp(-\pi s/2\alpha)\,\mathrm{d}s}{\sqrt{\cosh s - \cosh\lambda}} = \frac{\pi}{x\sqrt{xr_0}\alpha^2} Q_{\nu}(\cosh\lambda), \tag{60}$$

where $\nu = \pi/2\alpha - 1/2$ and $Q_{\nu}$ is the Legendre function of the second kind. This expression can be used to calculate the free-surface velocity Green function for any angles $\alpha \ll \lambda$, where $\lambda$ is defined by (43).

Consider the asymptotics behavior of $Q_{\nu}(\cosh\lambda)$ for small $\alpha$ ($\nu \gg 1$) and finite $\lambda$. For $\lambda > \log\sqrt{2}$ the asymptotic of the Legendre function is given by [19, Equation 8.723.2]:

$$Q_{\nu}(\cosh\lambda) \sim \sqrt{\pi} \frac{\Gamma(\nu+1)}{\Gamma(\nu+3/2)} \frac{\mathrm{e}^{-(\nu+1)\lambda}}{(1-\mathrm{e}^{-2\lambda})^{1/2}}\, {}_2F_1\left(\frac{1}{2}; \frac{1}{2}; \nu + \frac{3}{2}; \frac{1}{1-\mathrm{e}^{2\lambda}}\right), \tag{61}$$

where ${}_2F_1$ denotes the hypergeometric function. For large $\nu$ it behaves as [20, Equation 2.3.2.10]:

$$ {}_2F_1\left(\frac{1}{2};\frac{1}{2};\nu+\frac{3}{2};\frac{1}{1-\mathrm{e}^{2\lambda}}\right)\sim 1+\frac{(1/2)(1/2)}{\nu+3/2}\frac{1}{1-\mathrm{e}^{2\lambda}}, \tag{62}$$

Estimating the ratio $\Gamma(\nu+1)/\Gamma(\nu+3/2)$ as $\nu^{-1/2}$, for small $\alpha$ we obtain:

$$W\sim\frac{\pi}{x}\sqrt{\frac{1}{xr_0\sinh\lambda}}\frac{\mathrm{e}^{-\pi\lambda/2\alpha}}{\alpha^{3/2}} \tag{63}$$

It is seen now that for small angles $\alpha$ the free-surface velocity Green function exhibits a boundary layer behavior with an exponential decay.

For small $x$ the parameter $\lambda$, defined by (43), is large. In such a case the asymptotic behavior of the Legendre function is given by a relation [19, Equation 8.766.2]:

$$Q_\nu(\cosh\lambda)\sim\frac{\sqrt{\pi}}{2}\frac{\Gamma(\nu+1)}{\Gamma(\nu+3/2)\cosh^{\nu+1}\lambda}, \tag{64}$$

which leads to the following asymptotic expression for the free-surface velocity Green function:

$$W\sim\frac{2\pi^{3/2}}{r_0^2\alpha^2}\frac{\Gamma(\nu+1)}{\Gamma(\nu+3/2)}\frac{\xi^{\pi/2\alpha-1}}{\left(1+\eta^2\right)^{\pi/2\alpha+1/2}}. \tag{65}$$

Here $\xi=x/r_0$ and $\eta=y/r_0$. Thus, near the shore line ($x\ll 1$) for any $\alpha<\pi/2$ the free-surface velocity $W$ decays to zero; for $\alpha=\pi/2$ it is finite, and for $\pi/2<\alpha\leq\pi$ it is singular (compare with Equation 30).

### 4.5. Numerical examples

We conclude this section by some numerical examples. The integrand of (55) is a smooth function, except at the lower limit of integration, where it contains an integrable singularity. In our computations this point was isolated in the small vicinity of $\lambda$, where the integration was performed analytically. The remaining integral was computed by using the Romberg scheme.

Figure 5a is a comparison between the computed results of the surface velocity by invoking (54) and (59) which appears to be in a good agreement. In Figure 5b the same data are compared against the asymptotic solution (60) where it is shown that for small sloping angles the asymptotic expression is quite accurate. In Figure 6, a 3D plot of the free-surface velocity is shown. It is seen that the free surface velocity decays exponentially with respect to small $\alpha$ and small $x$. Its maximum appears approximately above the source.

## 5. Curved basins

We consider in the sequel two basic types of curved basins: a cylindrical basin with a semi-circular cross section, and an hemi-spherical basin.

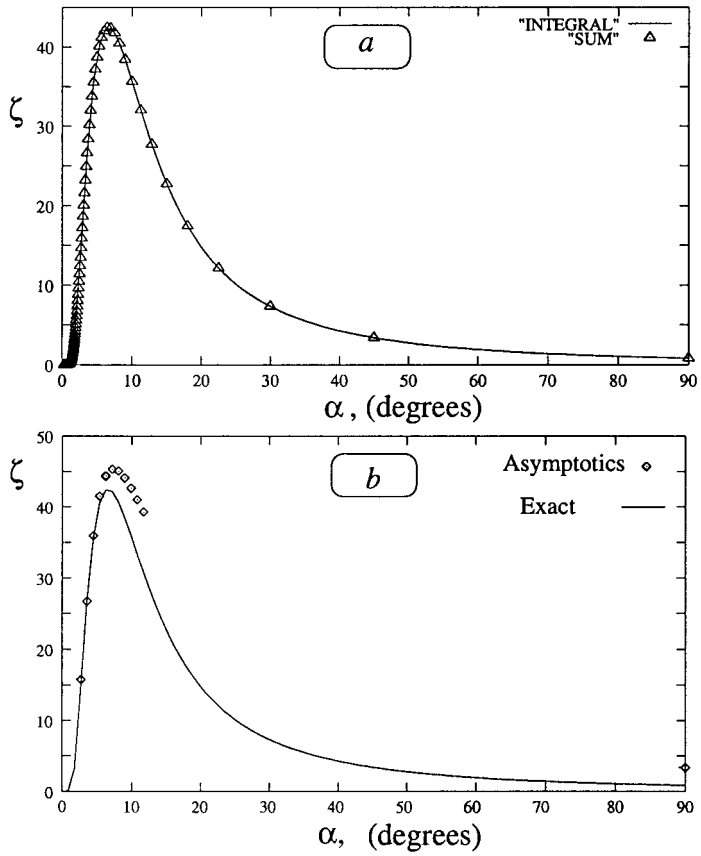


*Figure 5.* Free-surface velocity $\zeta = Wr_0^2/Q_0$ for a source $Q_0$ located at $\xi = x/r_0 = 0{\cdot}88$, $\eta = y/r_0 = 0$. Solid line: numerical integration of the integral representation (54) which is valid for any $\alpha$. Symbols: (a) finite sum (21) which is valid for $\alpha = \pi/2n$, $n$-integer; (b) asymptotic expressions.

### 5.1. THE SEMI-CIRCULAR CYLINDRICAL BASIN

We derive the solution for a special cylindrical basin: the cross-section is a semi-circle of radius $a$. The $y$ axis is directed along the axis of the infinitely long cylinder. We introduce $\theta$ as the angle in cylindrical coordinates $(r, \theta, y)$ where $x$ and $z$ are represented by (32). We will consider a source in the point $(x_0, y_0, z_0) = (a\cos\theta_0, 0, -a\sin\theta_0)$. The Green function is composed of the following three contributions:

$$G(x, y, z; x_0, 0, z_0) = -\sum_{m=0}^{1} \frac{(-1)^m}{\sqrt{(x-x_0)^2 + y^2 + [z-(-1)^m z_0]^2}} + H(x, y, z; x_0, 0, z_0). \quad (66)$$

The function $H$ is regular and harmonic for $r \leq a$. We choose to express it in such a form that $H = 0$ for $z = 0$ ($\theta = 0$):

$$H(x, y, z; x_0, 0, y_0) = \sum_{n=1}^{\infty} \sin n\theta \int_0^{\infty} A_n(k) I_n(kr) \cos ky \, \mathrm{d}k. \quad (67)$$

Here $I_n$ denotes the modified Bessel function of the first kind and of order $n$. The coefficients $A_n$ are to be chosen to satisfy the boundary condition:

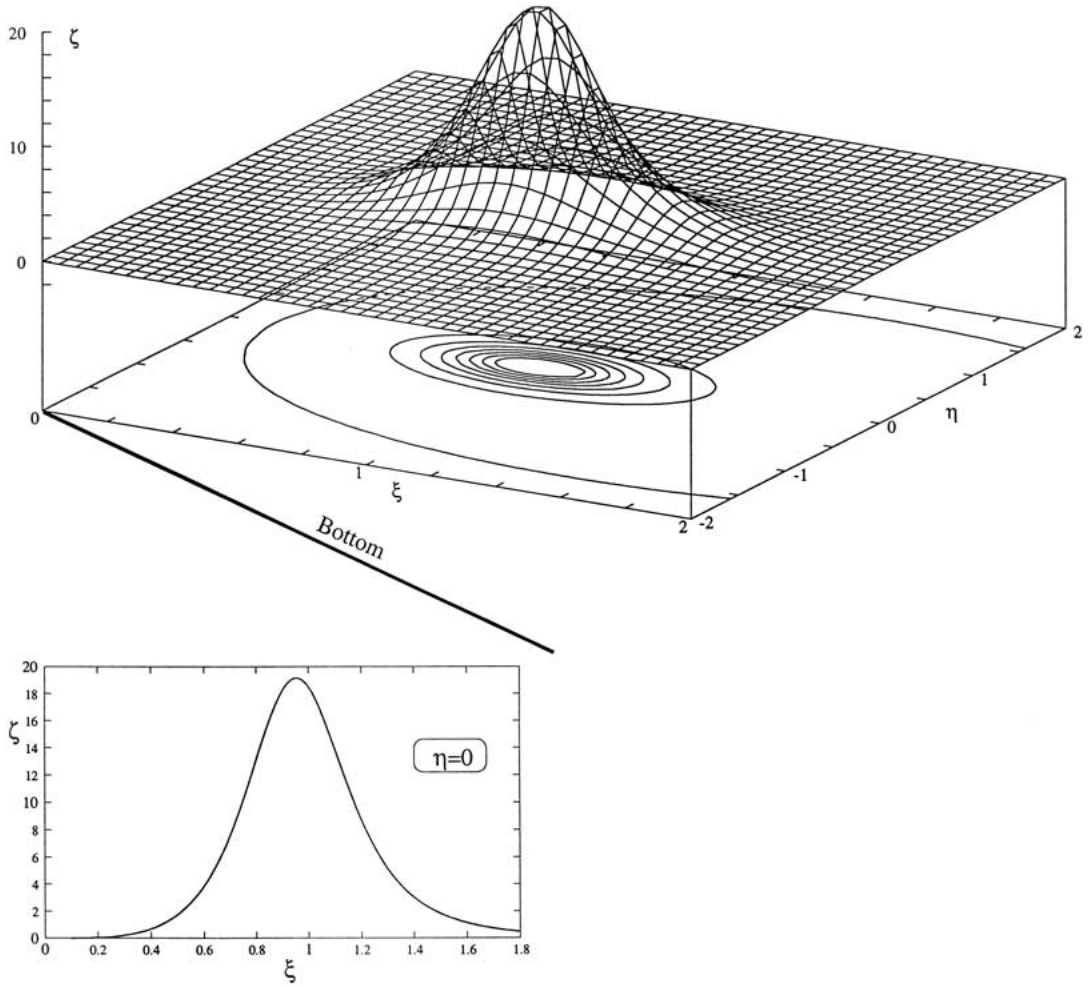


*Figure 6.* Free-surface velocity $\zeta = Wr_0^2/Q_0$ for a source of strength $Q_0$ as a function of $\xi = x/r_0$ and $\eta = y/r_0$: $(\alpha = \pi/10 = 18^\circ)$.

$$\frac{\partial H}{\partial r} = \frac{\partial}{\partial r}\left(\frac{1}{R^-} - \frac{1}{R^+}\right)_{r=a}, \tag{68}$$

where

$$\frac{1}{R^\mp} = \frac{1}{\sqrt{(x-x_0)^2 + (y-y_0)^2 + (z \mp z_0)^2}}. \tag{69}$$

To express (69) in an integral form, a well-known expansion can be applied:

$$\frac{1}{R^\mp} = \frac{2}{\pi}\int_0^\infty K_0\left[k\sqrt{(x-x_0)^2 + (z \mp z_0)^2}\right]\cos ky \, \mathrm{d}k \tag{70}$$

Next, we use the addition theorem for Bessel functions, valid for $r \leq a$:

$$K_0\left[k\sqrt{(x-x_0)^2 + (z \mp z_0)^2}\right] = \sum_{n=0}^{\infty} \epsilon_n \cos n(\theta \mp \theta_0) J_n(kr) K_n(ka). \tag{71}$$

where $\epsilon_n = 1$ for $n = 0$, $\epsilon_n = 2$ for $n > 0$, and $J_n$ denotes the Bessel function of the first kind. Application of the Neumann boundary conditions (68) and the orthogonality properties finally leads to:

$$G(x, y, z; x_0, 0, z_0) = -\sum_{m=0}^{1} \frac{(-1)^m}{\sqrt{(x-x_0)^2 + y^2 + [z-(-1)^m z_0]^2}} + \frac{4}{\pi} \sum_{n=1}^{\infty} \epsilon_n \sin(n\theta) \sin(n\theta_0) \int_0^{\infty} \frac{I_n(kr) J_n'(ka) K_n(ka)}{I_n'(ka)} \cos ky \, \mathrm{d}k, \tag{72}$$

where the prime ($'$) denotes differentiation with respect to the argument. The normal derivative of $G$ at the free surface is then given by:

$$W(x, y; x_0, 0, z_0) = -\frac{2z_0}{\left[(x-x_0)^2 + y^2 + z_0^2\right]^{3/2}} + \frac{8}{\pi x} \sum_{n=1}^{\infty} \mathrm{sgn}^{n+1}(x) \, n \sin(n\theta_0) \int_0^{\infty} I_n(kx) \frac{J_n'(ka)}{I_n'(ka)} K_n(ka) \cos ky \, \mathrm{d}k. \tag{73}$$

It should be noted that the above integral is non-singular for $x = 0$ (shore-line).

### 5.2. The hemi-spherical basin

As a final example we derive the solution for a hemispherical basin of radius $a$ where the undisturbed free surface is given by $z = 0$. We introduce spherical coordinates $(R, \theta, \phi)$ by defining:

$$z = R \cos\theta, \quad x + \mathrm{i}y = R \, \mathrm{e}^{\mathrm{i}\phi} \sin\theta, \tag{74}$$

where $R$ denotes the radial spherical coordinate. Since $z < 0$, the range of variation in the fluid domain is $\pi/2 < \theta < \pi$ and $0 < \phi < 2\pi$.

Let us consider a source located on the hemi-sphere at the point $(x_0, y_0, z_0)$. The Green function is composed of three contributions:

$$G(x, y, z; x_0, y_0, z_0) = -\frac{1}{R^-} + \frac{1}{R^+} + H(x, y, z; x_0, y_0, z_0). \tag{75}$$

Here $H$ is regular and harmonic for $R \leq a$. It obeys the condition $H(x, y, 0; x_0, y_0, z_0) = 0$. On the impermeable spherical wall we have the boundary condition:

$$\frac{\partial H}{\partial R} = \frac{\partial}{\partial R}\left(\frac{1}{R^-} - \frac{1}{R^+}\right). \tag{76}$$

We express the source field and its image in terms of the Legendre functions [21]:

$$\frac{1}{R^{\mp}} = \sum_{n=0}^{\infty} \sum_{m=1}^{n} \epsilon_n \frac{(n-m)!}{(n+m)!} \frac{R^n}{a^{n+1}} P_n^m(\cos\theta) P_n^m(\pm\cos\theta_0) \cos m(\phi - \phi_0) \tag{77}$$

$$= \frac{1}{\sqrt{R^2 + a^2 - 2aR(\pm\cos\theta\cos\theta_0 + \sin\theta\sin\theta_0\cos(\phi - \phi_0))}}, \tag{78}$$

Using (77), the boundary condition (76) can be expressed as:

$$\begin{aligned}\frac{\partial}{\partial R}\left[\frac{1}{R^-}-\frac{1}{R^+}\right]_{R=a} &= \frac{2}{a^2}\sum_{n=0}^{\infty}\sum_{m=1}^{n} n\frac{(n-m)!}{(n+m)!}\\ &\quad\times P_n^m(\cos\theta)\left[P_n^m(\cos\theta_0)-P_n^m(-\cos\theta_0)\right]\cos m(\phi-\phi_0)\\ &= \frac{2}{a^2}\sum_{n=0}^{\infty}\sum_{m=1}^{n} n\frac{(n-m)!}{(n+m)!}\left[1-(-1)^{n-m}\right]\\ &\quad\times P_n^m(\cos\theta)P_n^m(\cos\theta_0)\cos m(\phi-\phi_0).\end{aligned} \tag{79}$$

For $H(x, y, z; x_0, y_0, z_0)$ we select a general interior spherical harmonic given by:

$$\begin{aligned}H(R,\theta,\phi;a,\theta_0,\phi_0) = &\sum_{n=0}^{\infty}\sum_{m=1}^{n}\epsilon_n\frac{(n-m)!}{(n+m)!}\left[1-(-1)^{n-m}\right]\\ &\times\frac{R^n}{a^{n+1}}P_n^m(\cos\theta)P_n^m(\cos\theta_0)\cos m(\phi-\phi_0),\end{aligned} \tag{80}$$

which clearly satisfies (76) and $H(R, \pi/2, \phi; a, \theta_0, \phi_0) = 0$. Since $(\mathrm{d}/\mathrm{d}\mu)P_n^m(\mu)|_{\mu=0} = -(n-m+1)P_{n+1}^m(0)$, its normal derivative at the free surface is found as:

$$\begin{aligned}W(x, y; x_0, 0, z_0) = &-\frac{2z_0}{((x-x_0)^2+y^2+z_0^2)^{3/2}}\\ &-2\sum_{n=0}^{\infty}\sum_{m=1}^{n}\frac{\epsilon_n(n-m+1)!}{(n+m)!}\frac{[1-(-1)^{n-m}]R^{n-1}}{a^{n+1}}\\ &\times P_n^m(0)P_n^m(\cos\theta_0)\cos m(\phi-\phi_0).\end{aligned} \tag{81}$$

It is also possible to express $P_n^m(0)$ in terms of the Gamma function [19, p. 1009].

## 6. Concluding remarks

Some basic Green functions for impulsive tsunami generation in three dimensions have been derived analytically. The equipotential condition is assumed to be valid at the free surface throughout the tsunami generation process. This requires a time scale shorter than the gravitational time scale for the local depth.

Rectangular geometries have been treated by using the image method. There is also an image solution given by $n$ sources plus $n$ sinks for a uniform sloping beach of angle $\pi/(2n)$, where $n$ is a positive integer. The connection between this particular simple solution and the general integral solution, which is valid for any slope, has been analytically established. It is interesting to note that the impulsive Green function for a uniform slope decays exponentially to zero both for small $\alpha$ and small $x$. We have analyzed three more complicated cases: a beach with an arbitrary slope angle, a semi-cylindrical basin with a circular cross-section, and a hemi-spherical basin.

We have introduced the time-dependent bottom deflection $\chi(x, y, z, t)$ measured in the normal direction. Our linearized theory implies that the vertical velocity at the initially horizontal bottom is given by $w = \partial\chi/\partial t$. A second-order nonlinear condition on such a bottom could be given by: $w = \partial\chi/\partial t + \nabla\cdot(\chi\nabla_H\Phi)$, where $\nabla_H$ denotes the horizontal gradient operator.

From this condition one might evaluate the leading nonlinear correction to the linearized bottom condition, assuming that the impulsive bottom deflection $\chi(x, y, z, t)$ is specified. However, in the present work we are only concerned with impulsive Green functions for the fully linearized problem. The incorporation of weak nonlinearities at the bottom is left for future work.

## References


1. P. A. Tyvand and A. R. F. Storhaug, Green functions for impulsive free-surface flows due to bottom deflections in two-dimensional topographies. *Phys. Fluids* 12 (2000) 2819–2833.
2. T. Miloh and P. A. Tyvand, Non-linear transient free surface flow and dip formation due to a point sink. *Phys. Fluids* A 5 (1993) 1368–1375.
3. M. Xue and D. K. P. Yue, Nonlinear free-surface flow due to an impulsively started submerged point sink. *J. Fluid Mech.* 364 (1998) 325–347.
4. B. T. Lubin and G. S. Springer, The formation of a dip on the surface of a liquid draining from a tank. *J. Fluid Mech.* 29 (1965) 385–390.
5. Q.-N. Zhou and W. P. Graebel, Axisymmetric draining of a cylindrical tank with a free surface. *J. Fluid Mech.* 221 (1990) 511–532.
6. P. A. Tyvand, Unsteady free-surface flow due to a line source. *Phys. Fluids* A 1 (1992) 671–676.
7. M. Landrini and P. A. Tyvand, Generation of water waves and bores by impulsive bottom flux. *J. Eng. Math.* 39 (2001) 131–170.
8. T. Miloh, A note on impulsive sphere motion beneath a free-surface. *J. Eng.Math*. 41 (2001) 1–11.
9. E. O. Tuck and H.-L. San, Long wave generation on a sloping beach. *J. Fluid Mech.* 51 (1972) 449–461.
10. P. C. Sabatier, On the water waves produced by ground motion. *J. Fluid Mech*. 126 (1983) 27–58.
11. J. N. Newman, The approximation of the free surface Green functions. In: P. A. Martin and G.R. Wickham (eds.), *Proc. of Ursell's Retirement Meeting: Wave Asymptotics*. Cambridge (UK): Cambridge Univ. Press (1992) 107–132.
12. J. L. Hammack, A note on tsunamis: their generation and propagation in an ocean of uniform depth. *J. Fluid Mech.* 60 (1973) 769–799.
13. J. N. Newman, *Marine Hydrodynamics*. Cambridge (Mass.): MIT Press (1977) 402 pp.
14. G. Zilman and T. Miloh. Hydrodynamics of a body moving over a mud layer–Part I: Wave resistance. *J. Ship Research* 39 (1995) 194–201.
15. A. E. H. Love, *A Treatise on the Mathematical Theory of Elasticity*. New York: Dover (1944) 643 pp.
16. N. N. Lebedev, I.P. Skalskaya and Y.S. Uflyand, *Problems of Mathematical Physics*. Englewood Cliffs, N.J.: Prentice-Hall (1965) 429 pp.
17. A. P. Prudnikov, Yu. A. Brychkov and O. I. Marichev, *Integral and Series*, Vol. 1. New York: Gordon and Breach, (1988) 797 pp.
18. H. Bateman and A. Erdélyi, *Tables of Integral Transforms*, Vol. 1. New York: Mc. Graw-Hill (1954) 391 pp.
19. I. S. Gradshteyn and I.M. Ryzhik, *Tables of Integrals, Series and Products*. New York: Academic Press (1965) 1160 pp.
20. H. Bateman and A. Erdélyi, *Higher Transcendental Functions*, Vol. 1. New York: Mc. Graw-Hill (1953) 302 pp.
21. E. N. Hobson, *The Theory of Spherical and Ellipsoidal Harmonics*. New York: Chelsea Publ. Comp. (1965) 500 pp.